European Polymer Journal 98 (2018) 83–93

Contents lists available at ScienceDirect

European Polymer Journal

journal homepage: www.elsevier.com/locate/europolj

Synthesis, characterization and stereocomplexation of polyamide 11/polylactide diblock copolymers

Lorenza Gardella[a,*], Rosica Mincheva[b,**], Julien De Winter[c], Yuya Tachibana[d], Jean-Marie Raquez[b], Philippe Dubois[b], Orietta Monticelli[a]

[a] Dipartimento di Chimica e Chimica Industriale, Università di Genova, Via Dodecaneso, 31, 16146 Genova, Italy
[b] Laboratory of Polymeric and Composite Materials, Center of Innovation and Research in Materials and Polymers (CIRMAP), University of Mons-UMONS, Place du Parc 20, B-7000 Mons, Belgium
[c] Organic Synthesis and Mass Spectrometry Laboratory, Interdisciplinary Center for Mass Spectrometry (CISMa), Center of Innovation and Research in Materials and Polymers (CIRMAP), University of Mons-UMONS, Place du Parc 23, B-7000 Mons, Belgium
[d] Division of Molecular Science, Faculty of Science and Technology, Gunma University, 1-5-1 Tenjin, Kiryu, Gunma 376-8515, Japan

ARTICLE INFO

Keywords:
Polyamide 11
Polylactide
Biopolymer
Diblock copolymer
Stereocomplexation

ABSTRACT

The present work deals with the building of novel, fully bio-based polyamide 11 (PA11)/polylactide (PLA) diblock copolymers ($PA11_xPLA_y$). The adopted two-step synthetic strategy involves first the preparation of an amino-terminated PA11 prepolymer (*i.e.*, having the amino end-group available and the carboxylic one protected), to be employed subsequently as a macro-initiator in the ring-opening polymerization of D-lactide (or L-lactide). Upon tuning the lactide conversion, diblock copolymers with different PA11/PLA ratios are targeted and achieved, as demonstrated by ^{1}H NMR and TGA analysis. The thermal properties of these double-crystalline polymers are characterized by means of DSC. Finally, fast stereocomplexation is demonstrated upon mixing the enantiomeric $PA11_xPLA_y$ diblock pairs. Indeed, the idea behind these systems is to conjugate the properties of PLA with those of the high-performance PA11, in a cumulative rather than intermediate fashion, as for widely reported random poly(ester amide)s, but without phase separation occurring, which is the case for PLA/PA11 immiscible blends. In addition, the presence of the stereocomplex, well-known for its improved chemical/thermal resistance over PLA homopolymer, could impart even further quality to the final materials.

1. Introduction

Polylactide (PLA) and polyamide 11 (PA11) are both thermoplastic, bio-based polymers, with PA11 featuring superior thermal and mechanical properties compared to PLA [1,2]. Blends of the two, with the more-costly (and non-biodegradable) high-performance PA11 as the minority partner, have been pursued, because of the potential to have a system 100% derived from renewable sources where the PLA matrix benefits from the high thermal stability and high impact properties of PA11 [3–7]. Unfortunately, the immiscible nature of the two polymers, resulting in a drop-matrix morphology, prevents the actual obtainment of good/improved material properties for end-use applications, thereby requiring further compatibilization work to be done (moreover, not always with satisfactory outcome) [4–7]. Random copolymers of PLA/PA11 have also been prepared by melt polycondensation route, with the main result to tune the crystallinity of the prevailing component, the minor one acting as a constitutional defect [8,9]. Indeed, aliphatic poly (ester-amide)s, typically displaying a random distribution of ester and amide groups in the main chain, are a class of polymers having found increased interest and development in the recent years, by virtue of their combination of properties: the hydrolytically-degradable ester bonds impart good degradability (besides reducing the overall extent of crystallinity), while the hydrogen bonds developed by the amide groups strengthen the resulting materials [10–12]. It is worth mentioning that co-poly(ester-amide)s are further known for their remarkable thermal/thermo-mechanical properties even at relatively low molecular weight [12].

As an option, this work comes up with the design of PA11/PLA block copolymers, whereby both polymer components could keep/express their own specific properties (for example, other than because of its superior thermal and mechanical properties, PA11 is highly appealing also because, in its melt-quenched δ′-form, it exhibits ferroelectricity, piezoelectricity, and pyroelectricity) [13,14], without any phase segregation on a macroscopic scale occurring. Therefore, efforts

* Corresponding author.
** Corresponding author.
E-mail addresses: lorens85@gmail.com (L. Gardella), Rosica.MINCHEVA@umons.ac.be (R. Mincheva).

https://doi.org/10.1016/j.eurpolymj.2017.11.008
Received 20 June 2017; Received in revised form 15 October 2017; Accepted 2 November 2017
Available online 04 November 2017
0014-3057/

were conveyed towards the preparation of $PA11_xPLA_y$ – either poly(D-lactide) (PDLA) or poly(L-lactide) (PLLA) – di-block copolymers with variable PA11/PLA ratios, whose structure and structuring were then studied. Furthermore, stereocomplexation was expected to occur upon mixing the $PA11_xPDLA_y$/$PA11_xPLLA_y$ enantiomeric pairs,[15] to afford stereocomplex-PLA-based materials reinforced by the dispersed, tougher PA11 domains (or *viceversa* – the melting temperature of the stereocomplex being higher than that of PA11).

2. Experimental

2.1. Materials

11-aminoundecanoic acid (purity 97%) and dodecylamine (purity 98%) were purchased from Sigma-Aldrich and Acros Organics™, respectively, and used without further treatments. L-lactide (L-LA, Purasorb® L) and D-lactide (D-LA, Purasorb® D) with optical purity > 99.5% (MW = 144 g/mol, free acid < 1 meq/kg, water content < 0.02%) were supplied by Purac Biochem BV (The Netherlands) and stored in a glove box prior to use. ULTRANOX® 626 [bis (2,4-di-t-butylphenyl) pentaerythritol diphosphite, GE Specialty Chemicals] was dried at room temperature in vacuum-oven before each usage. Tin(II) 2-ethylhexanoate [$Sn(Oct)_2$] (95%; Sigma-Aldrich) and trifluoroacetic anhydride (TFAA; ≥99%, Sigma-Aldrich) were used as received. Toluene and dichloromethane were dried using an MBraun solvent purification system under N_2 flow; all other solvents [*i.e.*, methanol, chloroform and 1,1,1,3,3,3-hexafluoro-2-propanol (HFIP), VWR] were analytical grade and used as received.

2.2. Synthesis of (amino-terminated) polyamide 11 (PA11)

Amino-terminated polyamide 11 was synthesized by self-condensation (amidation) reaction of 11-aminoundecanoic acid using dodecylamine as a(n) (amino) chain-terminating agent.

In details, 50 g of 11-aminoundecanoic acid were charged, together with 0.86 g of dodecylamine, into a 250-mL specially designed and adapted Inox® Autoclave reactor (Autoclave-France, France) equipped with a mechanical stirrer; the autoclave was closed and flushed with nitrogen for about 15 min. The system was then filled with nitrogen to a relative pressure of 2 bar and heated to 190 °C, at which temperature the reaction mixture (under stirring, at 50 rpm, throughout the reaction) was allowed to slowly melt for 15 min. The temperature was then raised to 200 °C and held there for 45 min, with the pressure maintained at 2 bar. Next, the pressure was gently lowered to atmospheric and the water produced was removed with the help of a slow nitrogen bleed, while cooling the steam to collect it as a condensate, till no more vapor evolved (that is, over a period of approximately 10 min). At this point, the temperature was further increased to 220 °C, and the polymerization carried out for 4 h at atmospheric pressure under vigorous flow of nitrogen. It was observed the stirring to become difficult in the very last half-an-hour of the reaction. The finished product was recovered by direct extrusion from a bottom hole in the autoclave on applying a nitrogen pressure: a slightly-greyish, opaque, fiber-forming and tough polymer was obtained, with a yield of ~90%.

The as-obtained polymer, crushed into small pieces, was "washed" with boiling methanol for 3 days using a Soxhlet apparatus, and finally dried in vacuum at 60 °C for further characterization and employment (PA11).

^{1}H NMR (3/1 v/v HFIP/$CDCl_3$) **dodecylamine**: δ = 0.73 [t, $CH_3(CH_2)_{11}NH_2$], 1.08–1.26 [m, $CH_3(CH_2)_9CH_2CH_2NH_2$], 1.5 [Q, $CH_3(CH_2)_9CH_2CH_2NH_2$], 2.85 [t, $CH_3(CH_2)_{10}CH_2NH_2$], 4.35–4.75 (m/s, HFIP), 7.08 (s, $CHCl_3$); **11-aminoundecanoic acid**: δ = 1.10–1.26 [m, $NH_2CH_2CH_2(CH_2)_6CH_2CH_2CO_2H$], 1.39 [Q, $NH_2CH_2CH_2(CH_2)_6CH_2CH_2CO_2H$], 1.45 [Q, $NH_2CH_2CH_2(CH_2)_6CH_2CH_2CO_2H$], 2.09 [t, $NH_2CH_2CH_2(CH_2)_6CH_2CH_2CO_2H$], 2.89 [t, $NH_2CH_2CH_2(CH_2)_6CH_2CH_2CO_2H$], 4.35–4.75 (m/s, HFIP), 7.08 (s, $CHCl_3$), 11 [s, $NH_2CH_2CH_2(CH_2)_6CH_2CH_2CO_2H$]; **PA11**: δ = 0.74 {t, $CH_3(CH_2)_9CH_2CH_2NH[COCH_2CH_2(CH_2)_6CH_2CH_2NH]_nCOCH_2CH_2(CH_2)_6CH_2CH_2NH_2$}, 1.10–1.26 {m, $CH_3(CH_2)_9CH_2CH_2NH[COCH_2CH_2(CH_2)_6CH_2CH_2NH]_nCOCH_2CH_2(CH_2)_6CH_2CH_2NH_2$}, 1.39 {Q, $CH_3(CH_2)_9CH_2CH_2NH[COCH_2CH_2(CH_2)_6CH_2CH_2NH]_nCOCH_2CH_2(CH_2)_6CH_2CH_2NH_2$}, 1.45 {Q, $CH_3(CH_2)_9CH_2CH_2NH[COCH_2CH_2(CH_2)_6CH_2CH_2NH]_nCOCH_2CH_2(CH_2)_6CH_2CH_2NH_2$}, 2.09 {t, $CH_3(CH_2)_9CH_2CH_2NH[COCH_2CH_2(CH_2)_6CH_2CH_2NH]_nCOCH_2CH_2(CH_2)_6CH_2CH_2NH_2$ – amide tautomer}, 2.19 {t, $CH_3(CH_2)_9CH_2CH_2NH[COCH_2CH_2(CH_2)_6CH_2CH_2NH]_nCOCH_2CH_2(CH_2)_6CH_2CH_2NH_2$ – imidic acid tautomer}, 2.89 {t, $CH_3(CH_2)_9CH_2CH_2NH[COCH_2CH_2(CH_2)_6CH_2CH_2NH]_nCOCH_2CH_2(CH_2)_6CH_2CH_2NH_2$}, 3.09 {q, $CH_3(CH_2)_9CH_2CH_2NH[COCH_2CH_2(CH_2)_6CH_2CH_2NH]_nCOCH_2CH_2(CH_2)_6CH_2CH_2NH_2$}, 4.35–4.75 (m/s, HFIP), 5.88 {t, $CH_3(CH_2)_9CH_2CH_2NH[COCH_2CH_2(CH_2)_6CH_2CH_2NH]_nCOCH_2CH_2(CH_2)_6CH_2CH_2NH_2$}, 7.08 (s, $CHCl_3$).

FTIR (in cm^{-1}) **11-aminoundecanoic acid**: 3300–2400 (broad, COO−H, stretching), 2921 and 2850 (CH_2, asymmetric/symmetric stretching), 1636 (C=O, stretching), 1495 (NH_2, bending), 1391 (C−N, stretching); **PA11**: 3305 (hydrogen-bonded N−H, stretching), 3079 (N−H, overtone of amide II mode), 2919 and 2850 (CH_2, asymmetric/symmetric stretching), 1637 (C=O, stretching), 1540 (N−H, bending and C−N, stretching), 1467 (CH_2, scissoring).

2.3. N-trifluoroacetylation of PA11

As polyamide 11 is insoluble in common and GPC-suitable organic solvents, for purposes of analysis, a small amount of PA11 was reacted with trifluoroacetic anhydride. Indeed, upon N-trifluoroacetylation reaction (Scheme 1) the hydrogen bonds are broken and the modified polyamide becomes readily soluble in many solvents, such as chloroform and tetrahydrofuran. According to the literature, the conversion is high and reproducible, with no degradation of the polymer taking place [16,17].

Qualitatively, the success of N-trifluoroacetylation reaction was assessed by FTIR spectroscopy, whereby the three characteristic amide NH bands disappeared from the spectra of the modified polymers (which is indicative of a high degree of substitution), and the carbonyl stretching band shifted to higher frequencies (from 1637 to 1718 cm^{-1}), in agreement with the conversion of the amide group into an imide one.

In details, 0.5 g of PA11 were suspended in ~50 mL of anhydrous dichloromethane in a 100-mL two-neck flask provided with a magnetic stir-bar. Then, 0.3 mL of TFAA (that is, mole excess of CF_3CO:CONH = 2:1) were added and the system, under nitrogen atmosphere, was stirred at room temperature for about 16 h, during which time the polymer dissolved and a clear, colorless solution was obtained. Next, the solvent was evaporated with rotavapor and further dried in vacuum-oven for 4 h. A colorless, gel-like sticky product was obtained, easily re-dissolvable in chloroform for SEC analysis.

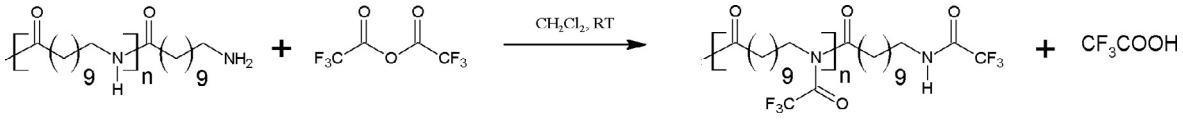

Scheme 1. N-trifluoroacetylation reaction of polyamide 11.

2.4. Synthesis of polyamide 11-poly(D-lactide) [or polyamide 11-poly(L-lactide)] di-block copolymers ($PA11_xPLA_y$)

Polyamide 11-poly(D-lactide) [or -poly(L-lactide)] diblock copolymers were synthesized by ring-opening polymerization (ROP) of D-lactide (or L-lactide), using the amino-terminated PA11 as macroinitiator and $Sn(Oct)_2$ as a catalyst, in bulk at 185 °C.

In a typical procedure, 3 g of PA11 (previously vacuum-dried at 60 °C for 48 h) and about 10 g of D-LA were introduced into a 50-mL specially designed and adapted Inox® Autoclave reactor (Autoclave-France, France), together with a small amount of the antioxidant ULTRANOX® 626 (~0.3 wt%, relative to lactide). The reactor was quickly closed and purged with nitrogen for about 15 min, sealed under nitrogen atmosphere (to a relative pressure of ~0.1 bar) and heated to 185 °C – stirring, at 50 rpm, was generally allowed when the temperature reached ~100 °C, melting temperature of the monomer – at which temperature the reaction mixture was allowed to melt/homogeneize for 15 min. At this point, a small volume of a freshly prepared solution of $Sn(Oct)_2$ in toluene was added (such that $[PA11\text{-}NH_2]/[Sn(Oct)_2]$ = 2.5, or 6.25, or 12.5) through a dedicated orifice in the autoclave. The reaction was carried out for 1 h (or 15 min), before collecting the product, either by spatula on opening the reactor or directly flowing out of the bottom hole (depending on the final molecular weight and amount of residual lactide).

The crude products were dissolved in a HFIP/chloroform mixture (approximately 1/1 v/v) and poured into an excess of cold methanol: after filtering and vacuum-drying to constant weight, the as-purified polymers were obtained in form of fibrous flakes or as compacted powders (depending on the molecular weight). A slightest yellowing was observed, generally increasing with the percentage of polyamide in the copolymer and, the PA11/PLA ratio being equal, with the reaction time.

Hereinafter, the prepared diblock copolymers are labeled as $PA11_xPDLA_y$ (or $PA11_xPLLA_y$, in the case of the sample obtained from L-LA polymerization), where the subscripts represent the weight percentage of the two constituents, as calculated from ^{1}H NMR data.

^{1}H NMR (3/1 v/v HFIP/$CDCl_3$) D-/L-**lactide**: δ = 1.54 (d, CH_3), 4.35–4.75 (m/s, HFIP), 4.95 (q, CH), 7.08 (s, $CHCl_3$); **PLA**: δ = 1.46 {d, $H[OCH(C\mathbf{H}_3)COOCH(C\mathbf{H}_3)CO]_nOCH(CH_3)CO_2H$}, 4.35–4.75 (m/s, HFIP), 5.06 {q, $H[OC\mathbf{H}(CH_3)COOC\mathbf{H}(CH_3)CO]_nOCH(CH_3)CO_2H$}, 7.08 (s, $CHCl_3$); **$PA11_xPLA_y$**: δ = 0.74 {t, $C\mathbf{H}_3(CH_2)_9CH_2CH_2NH[COCH_2CH_2(CH_2)_6CH_2CH_2NH]_n[COCH(CH_3)OCOCH(CH_3)O]_mH$}, 1.10–1.26 {m, $CH_3(C\mathbf{H}_2)_9CH_2CH_2NH[COCH_2CH_2(C\mathbf{H}_2)_6CH_2CH_2NH]_n[COCH(CH_3)OCOCH(CH_3)O]_mH$}, 1.39 {Q, $CH_3(CH_2)_9CH_2CH_2NH[COCH_2C\mathbf{H}_2(CH_2)_6CH_2CH_2NH]_n[COCH(CH_3)OCOCH(CH_3)O]_mH$}, 1.44–1.46 {d, $CH_3(CH_2)_9CH_2CH_2NH[COCH_2CH_2(CH_2)_6CH_2CH_2NH]_n[COCH(C\mathbf{H}_3)OCOCH(C\mathbf{H}_3)O]_mH$}, 2.09 {t, $CH_3(CH_2)_9CH_2CH_2NH[COC\mathbf{H}_2CH_2(CH_2)_6CH_2CH_2NH]_n[COCH(CH_3)OCOCH(CH_3)O]_mH$ – amide tautomer}, 2.19 {t, $CH_3(CH_2)_9CH_2CH_2NH[COC\mathbf{H}_2CH_2(CH_2)_6CH_2CH_2NH]_n[COCH(CH_3)OCOCH(CH_3)O]_mH$ – imidic acid tautomer}, 3.09 {q, $CH_3(CH_2)_9CH_2C\mathbf{H}_2NH[COCH_2CH_2(CH_2)_6CH_2C\mathbf{H}_2NH]_n[COCH(CH_3)OCOCH(CH_3)O]_mH$}, 4.35–4.75 (m/s, HFIP), 5.06 {q, $CH_3(CH_2)_9CH_2CH_2NH[COCH_2CH_2(CH_2)_6CH_2CH_2NH]_n[COC\mathbf{H}(CH_3)OCOC\mathbf{H}(CH_3)O]_mH$}, 5.88 {t, $CH_3(CH_2)_9CH_2CH_2N\mathbf{H}[COCH_2CH_2(CH_2)_6CH_2CH_2N\mathbf{H}]_n[COCH(CH_3)OCOCH(CH_3)O]_mH$}, 7.08 (s, $CHCl_3$).

FTIR (in cm^{-1}) D-/L-**lactide**: 3000–2930 (CH_3 and CH, asymmetric/symmetric stretching), 1753 (C═O, stretching), 1456 and 1380 (CH_3, asymmetric and symmetric bending), 1355 (CH, bending), 1268 and 1094 (C—O—C, asymmetric and symmetric stretching), 934 (COO, ring breathing); **PLA**: 2995–2875 (CH_3 and CH, asymmetric/symmetric stretching), 1748 (C═O, stretching), 1452 and 1381 (CH_3, asymmetric and symmetric bending), 1360 (CH, bending), 1182 and 1083 (C—O—C, asymmetric and symmetric stretching), 955 (CH_3, rocking), 867 (C—C, stretching); **$PA11_xPLA_y$**: 3305 (hydrogen-bonded N—H, stretching), 3085 (N—H, overtone of amide II mode), 3000–2850 (CH_3, CH_2, CH, asymmetric/symmetric stretching), 1755 (ester C═O, stretching), 1638 (amide C═O, stretching), 1542 (N—H, bending and C—N, stretching), 1466 (CH_2, scissoring), 1455 and 1382 (CH_3, asymmetric and symmetric bending), 1360 (CH, bending), 1183 and 1085 (C—O—C, asymmetric and symmetric stretching), 955 (CH_3, rocking), 870 (C—C, stretching).

2.5. Preparation of $PA11_{25}PDLA_{75}/PA11_{21}PLLA_{79}$ blend ($PA11_{23}LD_{77}$)

In order to study stereocomplexation, the samples $PA11_{25}PDLA_{75}$ and $PA11_{21}PLLA_{79}$ were melt-blended by means of a laboratory glass tube reactor provided with a mechanical stirrer (Heidolth, type RZR1).

In details, 1.5 g of each component (vacuum-dried at 40 °C for 48 h) were charged in the tube; the tube was vacuum-evacuated for 30 min, followed by 5 min flushing with argon; the vacuum/argon cycles were repeated three times so as to fully remove humidity and oxygen from the reaction system, which was kept under a continuous flow of argon in the following. The reactor was then placed in a controlled aluminum heating block (set at 230 °C) and the polymers allowed to melt for 5 min, before activating the stirring (at 60 rpm) for another 5 min. After this time, the mixing was stopped and the mixture cooled down by quickly dipping the tube into a water bath. Pieces of a brittle (cream-color, whereas the two starting materials were pretty white) solid were recovered upon breaking the tube with a hammer ($PA11_{23}LD_{77}$).

2.6. Measurements

FTIR spectra were recorded on a Bruker IFS66 spectrometer in the spectral range 400–4000 cm^{-1}.

^{1}H and ^{13}C NMR spectra were collected with a Varian NMR Mercury Plus at a frequency of 300 MHz and a Bruker AMX-500 at a frequency of 500 MHz instruments, respectively, in a 3/1 v/v HFIP/$CDCl_3$ solvent mixture solutions containing TMS as internal standard.

Size exclusion chromatography (SEC) was performed in $CHCl_3$ at 30 °C using an Agilent liquid chromatograph equipped with an Agilent degasser, an isocratic HPLC pump (flow rate = 1 mL/min), an Agilent autosampler (loop volume = 200 μL, solution conc. = 2.5 mg/mL), an Agilent-DRI refractive index detector and three columns: a PL gel 10 μm guard column and two PL gel Mixed-D 10 μm columns (linear columns for separation of MWPS ranging from 500 to 106 g/mol). Polystyrene standards were used for calibration.

Matrix-assisted Laser Desorption/Ionization Time-of-Fight (MALDI-ToF) experiments were conducted using a Waters QToF Premier mass spectrometer equipped with a Nd-YAG laser, operating at 355 nm with a maximum output of 66.3 μJ per surface unit delivered to the sample in 2.2 ns pulses at 50 Hz repeating rate. Time-of-Flight mass analyses were performed in the reflectron mode at a resolution of about 10k and the samples were analysed using trans-2-[3-(4-tertbutylphenyl)-2-methyl-prop-2-enylidene]-malononitrile (DCTB), as a matrix at 40 mg mL^{-1} solution in $CHCl_3$. Samples were dissolved in HFIP to obtain 1 mg mL^{-1} solutions. 5 μL of formic acid were added to the analyte solution to promote the ionization. Aliquots (1 μL) of those solutions were applied onto the target area already bearing the matrix crystals, and air-dried. For the recording of the single-stage MS spectra, the quadrupole (rf-only mode) was set to pass all the ions in the *m/z* range between 500 to 30.000, and they were transmitted into the pusher region of the time-of-flight analyser where they were mass analysed with 1 s integration time. Data were acquired in continuum mode until acceptable averaged data were obtained.

Thermal gravimetrical analysis (TGA) was performed with a Mettler-Toledo TGA 1 thermogravimetric analyzer. The weight loss was recorded upon heating the samples (having initial masses of ca. 10 mg) at 20 °C/min from 25 to 800 °C, under a flow of nitrogen of 80 ml/min. The referred temperatures of maximum degradation rate (T_{max}) were taken as the inflection point of the sigmoidal steps (*i.e.*, the maxima of the first-derivative curve).

Differential scanning calorimetry (DSC) measurements were performed with a Mettler-Toledo TC10A calorimeter calibrated with high

purity indium and operating under flow of nitrogen. The sample weight was about 5 mg and a scanning rate of 10 °C/min was employed in all the runs. The samples were heated from 0 °C to 230 °C, at which temperature the melt was allowed to relax for 1 min, then cooled down to −10 °C, and finally heated up again to 230 °C (second heating scan). The reported T_g (glass transition temperature), $T_{c(c)}$ (crystallization/cold crystallization temperature) and T_m (melting temperature) values were defined as the midpoints of the sigmoidal curve, minima of the exotherms and maxima of the endotherms, respectively. When indicated, the degree of crystallinity (X_c) was calculated by using ideal enthalpies of fusion of 189 J/g for polyamide 11, 93 J/g for PLA homocrystals and 142 J/g for the stereocomplex [15,18].

Wide-angle X-ray diffraction (WAXD) analyses were performed on a Siemens D5000 diffractometer using Cu-Kα radiation (wavelength: 1.5406 Å) at room temperature. The samples were step-scanned from 5° to 30° in 2θ with steps of 0.02° with fixed counting time of 4 s (40 kV, 30 mA).

3. Results and discussion

In this work, novel polyamide 11-poly(D-lactide) diblock copolymers with different PA11/PLA ratios were prepared, according to a two-stage strategy (schematically depicted in Scheme 2) involving first the synthesis of an amino-terminated (*i.e.*, having the amino terminal group available and the carboxylic one protected) PA11 pre-polymer, to be subsequently used as a macro-initiator in the second step ROP of D-lactide. While the PA11 segment was maintained constant, the length of the PDLA block was varied by tuning the lactide conversion. A polyamide 11-poly(L-lactide) diblock was also synthesized, for the purpose of blending it with its enantiomeric counterpart and thus evaluating stereocomplexation.

3.1. Synthesis and characterization of PA11

The synthesis of the amino-terminated PA11 was carried out by direct polyamidation of 11-aminoundecanoic acid as described in the Experimental Section (for a quick look, the reaction conditions are indicated over the reaction arrows in Scheme 2). Namely, a two/three-step procedure was followed, schematized as: melting/pre-condensation of the amino acid (with most of the water expelled, up to ~90% conversion) and polymerization (wherein, with the aid of a nitrogen stream to remove the little water produced, the molecular weight of the product strongly increases). Dodecylamine was used as a(n) (amino) chain-terminating agent to control the molecular weight, simultaneously producing an amino-terminated polymer without the need of a post-polymerization end-capping. The amino acid-to-dodecylamine ratio was adjusted so as to get a PA11 pre-polymer with a number average molecular weight (M_n) around $10 \cdot 10^3$ g/mol. By methanol extraction, only ~1.5 wt% of a white powder was separated from the reaction product (corresponding to a polyamide compound, as identified by FTIR – see next – thence to be attributed to low oligomers), whereas no traces of unreacted monomer were detectable.

The structure of the obtained polymer was characterized by means of FTIR and ^{1}H NMR spectroscopies. Indeed (see Fig. 1S, comparing the FTIR spectra of PA11 and 11-aminoundecanoic acid), upon polycondensation, three new bands appeared in the group frequency region (at 3304, 3079 and 1541 cm^{-1}). These bands belong to the hydrogen-bonded NH stretch, to a characteristic secondary amide NH overtone and to the amide NH bend, respectively, thereby confirming the polyamide nature of the material. Fig. 1 shows the ^{1}H NMR spectrum of PA11, where all the signals were assigned as expected for a dodecylamine-terminated polyamide "oligomer", which definitely enables assessing the obtainment of the desired product. By comparing the integral of one of the resonances for the methylene protons in the polyamide chain (typically peak **g**) with the integrated intensity of the signals of the proton groups at the chain ends (that is, peaks **a** or **f**), a M_n of ~$13 \cdot 10^3$ g/mol was estimated (Table 1), in good agreement with the theoretical value.

Upon N-trifluoroacetylation reaction (which procedure proved highly reproducible – for details see the Experimental Section), PA11 became soluble in chloroform, therefore it could be analysed by SEC, whereby the monomodal distribution of the molecular weights was ascertained (polydispersity around 2; Fig. 2S).

The MALDI-TOF mass spectrum (Fig. 3S) revealed the presence of macromolecules with a mass up to (at least) ~ $25 \cdot 10^3$ g/mol – no inference on M_n, nor on the polydispersity, was possible, due to the overestimation of low molecular mass ions for such a broad dispersity, close to 2, as the one obtained in a polycondensation process [19]. Most important, the spectrum showed one major distribution, corresponding to the expected 11-aminoundecanoic polymer initiated with the dodecylamine moiety, thus confirming that this latter was effectively terminating the majority of the chains.

Based on TGA (see Fig. 2b), on linear heating PA11 is stable up to ~410 °C (T_{max} ~ 480 °C), with a second, smaller step of weight loss (~0.4 wt%) around 560 °C, which is generally attributed to the decomposition of cross-linked structures formed on heating [20,21].

The DSC thermograms are shown in Fig. 4 (and the characteristic values reported in Table 2): on cooling from the melt at a rate of 10 °C/min, PA11 undergoes a sharp crystallization event (with peak at 168 °C), which, based on the literature, can be assigned to the formation of the triclinic/(pseudohexagonal) δ-form of polyamide 11, reversibly transforming into the triclinic α-form on cooling below the Brill transition temperature of ~100 °C [18]. On subsequent heating, PA11 displays a bimodal melting peak, with maximum at 189 °C. Assuming a melting enthalpy of 189 J/g for a 100% crystalline sample [18], the degree of crystallinity developed on cooling can be calculated to be ~30%. A broad and weak glass transition can be discerned around 45 °C. Indeed, the thermal properties of our PA11 are in perfect agreement with those commonly reported in the literature for polyamide 11 [18,20–22].

3.2. Evaluation of PA11/lactide miscibility

The miscibility of monomer and initiator in the initial liquid mixture is a key point for the ring-opening polymerization, requisite for a relatively fast initiation. Therefore, before proceeding with the second step towards the diblock copolymers, it was of utmost importance to check the behavior of the PA11 pre-polymer and LA monomer in the molten state.

This was accomplished by heating, to begin with, a 3/1 (w/w) mixture of D-lactide and PA11 in a flask placed in a heating mantle and provided with a magnetic stirrer and observing the changes while measuring the temperature inside the flask with a thermocouple. Unlike the neat PA11, whose melting becomes macroscopically visible just above 180 °C, in the presence of the liquid lactide (melting temperature ~ 100 °C) the small PA11 pieces were observed to start "dissolving" at about 160 °C, till the obtainment of a unique liquid phase at about 175 °C. Upon slow cooling, this liquid phase was found to be preserved up to about 140 °C, at which temperature the precipitation of the solid PA11 occurred. Indeed, these observations indicate that the molten lactide acts as a solvent for PA11. It is worth mentioning that this finding was further corroborated by the evidence acquired during the ring-opening-polymerization tests performed in the autoclave reactor – see the next section – that the PA11 pieces "liquefy" in the interval of 155–180 °C, as revealed by a strong increase of the stirring-speed at constant couple, whereas, based on calorimetric data (Fig. 4b), the neat polymer is fully molten just at 195 °C.

Conversely, it turned out that, for a 1/1 (w/w) mixture of D-lactide and PA11, solid PA11 pieces were still present, at least up to 190 °C.

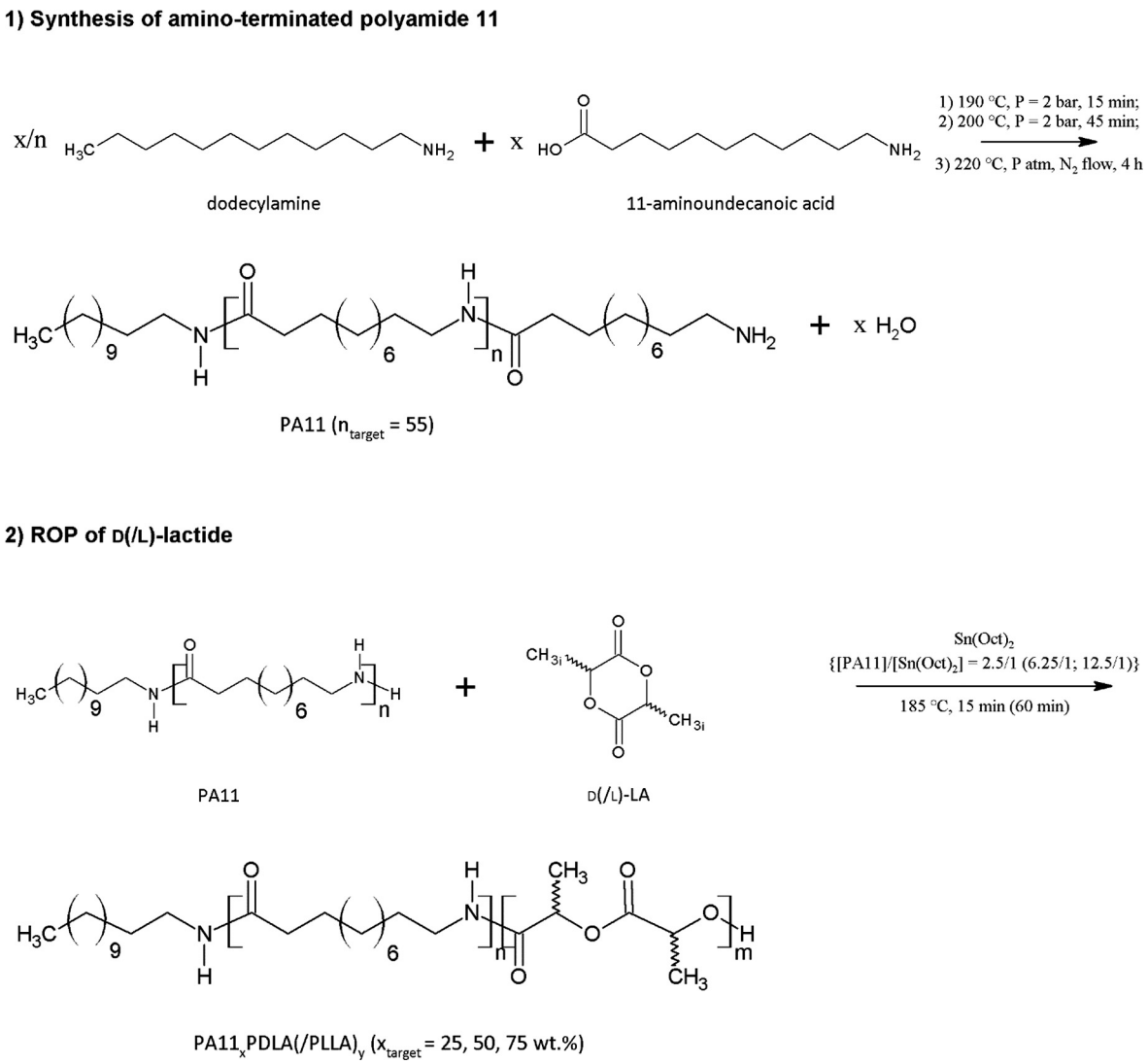

Scheme 2. Scheme of the adopted two-step synthetic strategy towards $PA11_xPLA_y$ diblock copolymers.

3.3. Synthesis and characterization of $PA11_xPLA_y$ diblock copolymers

The next goal of the work was the polymerization of D-lactide by aminolytic ROP induced from the amino terminal of the as-synthesized PA11, as depicted in Scheme 2. Ideally, one wanted to prepare $PA11_xPLA_y$ diblocks having different compositions: a PA11-rich (namely, PA11:PDLA = 75:25), a PLA-rich (namely, PA11:PDLA = 25:75) and a compositionally balanced (*i.e.*, containing ~ 50 wt% of each constituent) copolymers.

As detailed above, it was proven that, for a 3/1 (w/w) mixture of lactide and PA11, the molten lactide acts as a solvent for PA11, with the solubilization range being about 155–180 °C. Therefore, it was possible to employ a polymerization temperature of 185 °C (namely, below that of melting of PA11), which is a suitable one for the ROP of lactide, while ensuring that (at least at the beginning) the reaction system was perfectly homogeneous. On the other hand, as it turned out that, for a 1/1 (w/w) mixture, the amount of the lactide "solvent" was not enough to solubilize all PA11, all polymerizations were carried out from a LA/PA11 3/1 (w/w) supply – a slight excess of lactide was systematically added, with respect to this proportion, to compensate for eventual losses on opening the reactor to introduce the catalyst. Clearly, since the monomer-to-initiator ratio in the feed was fixed, the composition of the diblocks needed to be varied by acting on the lactide conversion.

At first, the ROP of D-LA was carried out using a $[PA11]/[Sn(Oct)_2]$ ratio of 2.5, for 1 h. FTIR analysis of the crude reaction product proved the occurred polymerization of D-LA to form PDLA, the conversion being quantitative, as inferable from the presence of the ester carbonyl stretching at 1754 cm^{-1}, whereas the characteristic band of lactide at 935 cm^{-1} had negligible magnitude (for reference, see the upper part of Fig. 1S) [23]. Likewise, on further shortening the polymerization to 15 min, with all other conditions being unchanged, it was observed that such a short time was still enough for the reaction to reach "completion" (*i.e.*, D-LA conversion ~ 96%, as evaluated by means of ^1H NMR spectroscopy). Therefore, two fibrous-like products with almost identical composition – based on the stoichiometry, a PA11:PDLA weight ratio close to 25:75 was expected – were obtained from the purification of these trials' output (see Fig. 4S – for the comments to TGA results refer to later on). As the sample produced over the one-hour polymerization was slightly discolored, whereas the one reacted for 15 min was pretty white (and it is know that side reactions become significant starting from the last stages of propagation, progressively broadening the molecular weight distribution), the subsequent characterizations where focused on this last one ($PA11_{25}PDLA_{75}$, from now on).

The FTIR spectrum of $PA11_{25}PDLA_{75}$ is shown in Fig. 2a, featuring both stretching bands of the amide and ester carbonyls, at 1637 cm^{-1} and 1754 cm^{-1}, respectively. This observation corroborates the dual polyamide 11/polylactide nature of the material, though not providing any information about the relation between the two constituents, either

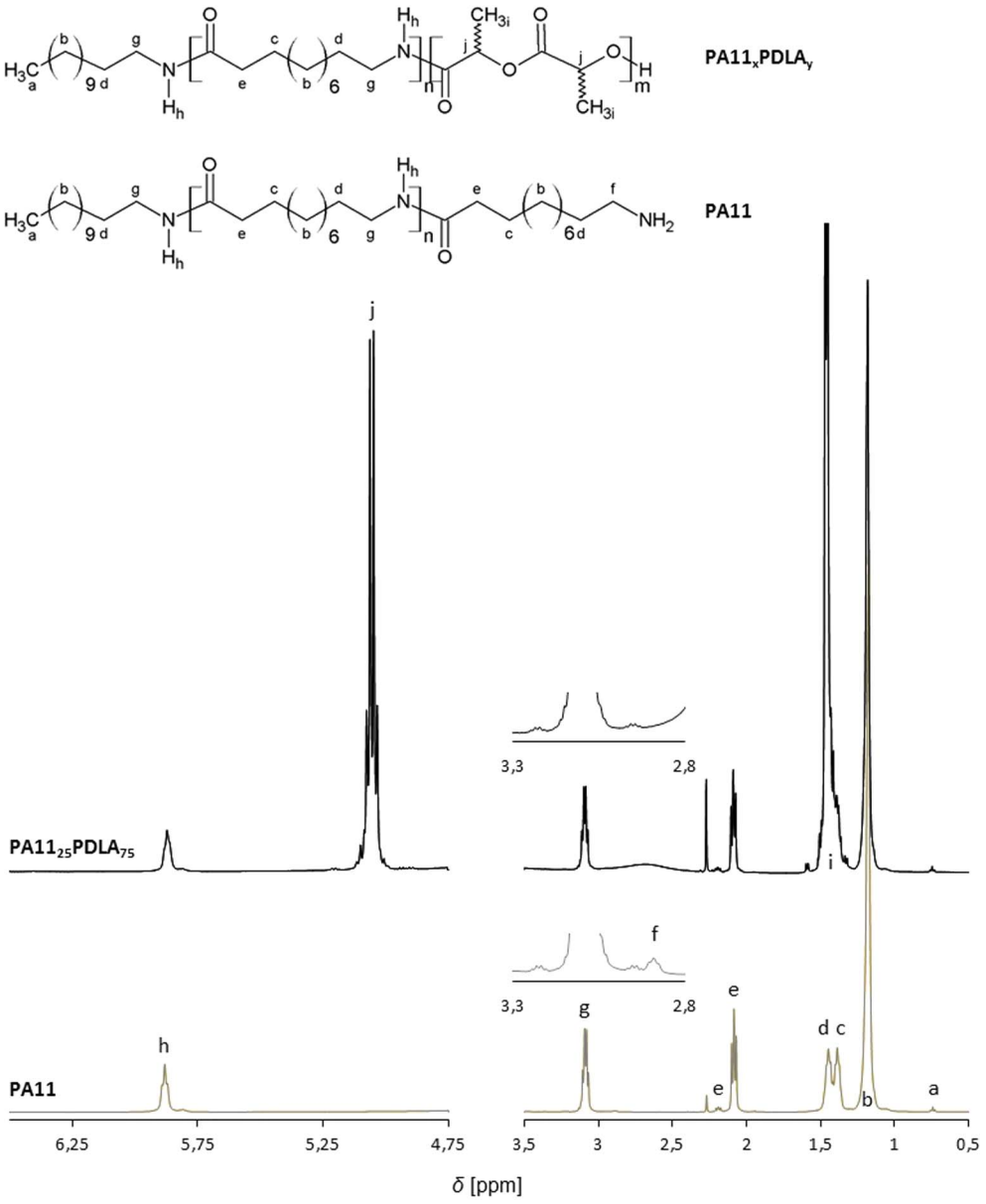

Fig. 1. ^{1}H NMR spectra of the PA11 pre-polymer and of the diblock sample $PA11_{25}PDLA_{75}$ in the regions at δ 6.5–4.75 and 3.5–0.5 ppm, with enlargement insets at δ 3.3–2.8 ppm.

Table 1
Molecular characteristics of the synthesized $PA11_xPLA_y$ diblock copolymer samples, together with the adopted ROP conditions (in bulk, at 185 °C).

Sample code	Monomer	[PA11] **[Sn(Oct)$_2$]**	ROP time [min]	Conversion[a] [%]	PA11:PLA (NMR)[b] [w:w]	PA11:PLA (TGA)[c] [w:w]	M_n[d,e] [10^3 g/mol]
PA11 (pre-polymer)							13[f]
$PA11_{25}PDLA_{75}$	D-LA	2.5	15	96	25:75	24:76	52[d], 54[e]
$PA11_{29}PLLA_{71}$	L-LA	2.5	15	90	29:71	28:72	45[d], 46[e]
$PA11_{45}PDLA_{55}$	D-LA	6.25	60	47	45:55	44:56	29[d], 30[e]
$PA11_{73}PDLA_{27}$	D-LA	12.5	60	19	73:27	74:26	18[d], 18[e]

[a] D-(/L-)-LA conversion estimated from the ^{1}H NMR spectra of the crude reaction products [by comparing the relative intensities of the resonance for the methine protons in the PLA chain (at δ 5.06 ppm – signal **j**), with that of the methine protons of the lactide monomer (typically at δ 4.95 ppm)].

[b] PA11:PLA weight ratio in the diblock, as determined by ^{1}H NMR spectroscopy [from the integral ratio of peaks **g** and **j**].

[c] PA11:PLA weight ratio in the diblock, as determined by TGA measurements [from the ratio of the two degradation steps].

[d] Numeric average molecular weight of the diblock, based on the PA11:PLA ratio determined by ^{1}H NMR spectroscopy, in the assumption that all PA11 and PLA are linked (calculated as: M_n [$*10^3$] = (13 * 100)/$PA11_{(NMR)}$, where 13 is the M_n of PA11 as determined by ^{1}H NMR, and $PA11_{(NMR)}$ is the wt.% of PA11, as determined by ^{1}H NMR).

[e] Numeric average molecular weight of the diblock, based on the PA11:PLA ratio determined by TGA measurements, in the assumption that all PA11 and PLA are linked (calculated as: M_n [$*10^3$] = (13 * 100)/$PA11_{(TGA)}$, where 13 is the M_n of PA11 as determined by ^{1}H NMR, and $PA11_{(TGA)}$ is the wt.% of PA11, as determined by TGA).

[f] Evaluated by ^{1}H NMR spectroscopy.

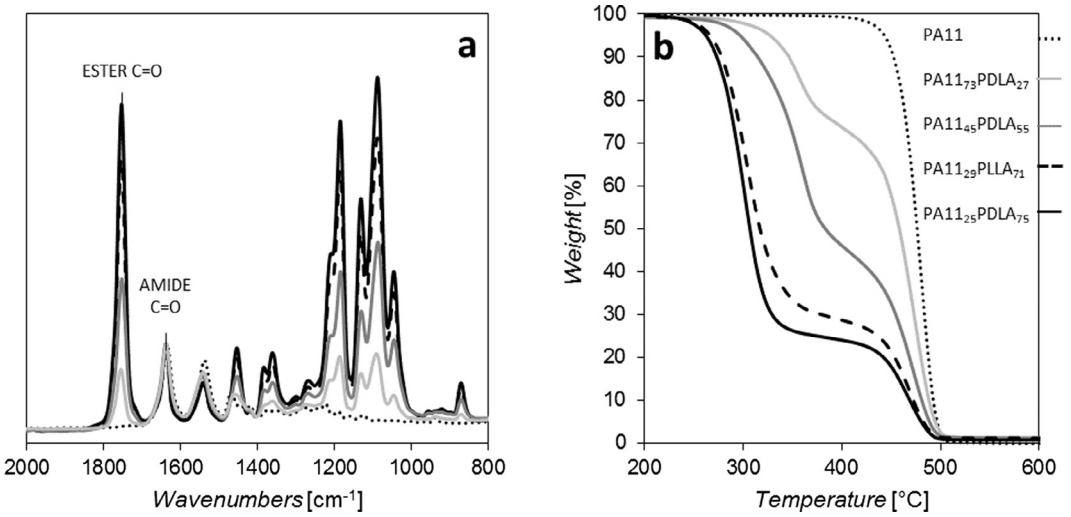

Fig. 2. FTIR spectra (a; spectra normalized with respect to PA11 carbonyl band at 1637 cm^{-1}), and TGA curves (b) of the synthesized $PA11_xPLA_y$ diblock copolymer samples – the traces of the PA11 pre-polymer (dotted lines) were included for the sake of comparison.

conjugated to form the desired diblock copolymer or simply blended as homopolymers. A first hint about the (at least partially) co-polymeric nature of our product was gained by dispersing a small amount of $PA11_{25}PDLA_{75}$ in chloroform, which resulted in fast sample "dis-aggregation", to give a slightly turbid solution containing several small gel-like particles. FTIR analysis on the (~10 wt%) product separated by filtration disclosed the presence of a (substantial, though smaller than the average – rough estimation: ~10–15 wt%) PLA fraction besides the predominant polyamide 11, the rest of which was in solution. Indeed, this result pointed out that the majority of PA11 (insoluble in chloroform) was actually covalently linked to the (chloroform-soluble) PLA segment. This inference was confirmed through ^{1}H NMR spectroscopy (see Fig. 1 – the spectrum of $PA11_{25}PDLA_{75}$ displays, together with the peaks of polyamide 11, those for the methyl and methine protons of PLA at δ 1.44–1.46 ppm and 5.06 ppm, respectively). In fact, the triplet of the α-amino methylene protons of (unbound) PA11 (signal **f**) is no more discernible at δ 2.9 ppm (whereas the terminal methyl proton signal **a** is still visible and its relative intensity unchanged). That is, the **f** resonance has shifted upon formation of amide linkages, predictably joining peak **g**. This evidence is indicative that the terminal amino functions of the PA11 pre-polymer effectively and quantitatively initiated the ROP of D-lactide. Eventually, from the ^{1}H NMR spectrum, based on the integration ratio of the peaks **g** and **j**, the PA11 and PDLA contents were calculated to be ~25 wt% and ~75 wt%, respectively (which is the exact proportions that have been targeted through the initial stoichiometry). Fig. 5S shows the ^{13}C NMR spectrum of the $PA11_{25}PDLA_{75}$ diblock copolymer in comparison to PA11. As might be seen, while the PA11 spectrum shows only the chemical shifts expected for PA11 in trans-form [24], new shifts at 16.16 and 172.11 ppm are observed for the diblock copolymer. These newly occurring shifts are reasonably ascribed to methyl and ester carbons from the PDLA block, respectively. The chemical shift at about 69 ppm for the methanetriyl group (R_3CH) of PLA does not occur, most probably due to overlapping with the HFIP carbon. A closer look to the carbonyl region of 170–180 ppm (Fig. 5S zoom) shows exclusively two diad signals from the PA11 carbonyl (178.35 ppm) and from the PLA ester carbons, hence suggesting the formation of a block structure [25]. Low intensity signals next to the PLA carbonyl might be explained with limited transesterification reactions during synthesis [25].

Since it had been observed that, using the aforementioned conditions, the reaction was too fast to lower the lactide conversion, thence get PA11-richer copolymers, by controlling the polymerization time, further tests were carried out, for 1 h, reducing the amount of the added catalyst of either a factor 2.5 or 5. As expected, FTIR analysis of both crude products, collected as (macroscopically) homogenous viscous liquids, revealed the presence of a big amount of unreacted lactide (*i.e.*, D-LA conversion ~47% and ~19%, respectively, as estimated by ^{1}H NMR spectroscopy). Accordingly, from the ^{1}H NMR spectra of the purified copolymers (Fig. 3), a PDLA content of ~55 wt% and ~27 wt % was determined (entries $PA11_{45}PDLA_{55}$ and $PA11_{73}PDLA_{27}$ in Table 1). Moreover, similar as in the case of the sample $PA11_{25}PDLA_{75}$, signal **f** disappeared from the spectra, which substantiates the co-polymeric nature of these materials as well.

Fig. 2a shows the FTIR spectra of the three copolymer samples produced ($PA11_{25}PDLA_{75}$, $PA11_{45}PDLA_{55}$ and $PA11_{73}PDLA_{27}$), whose different PA11/PLA content can be easily appreciated by comparing the

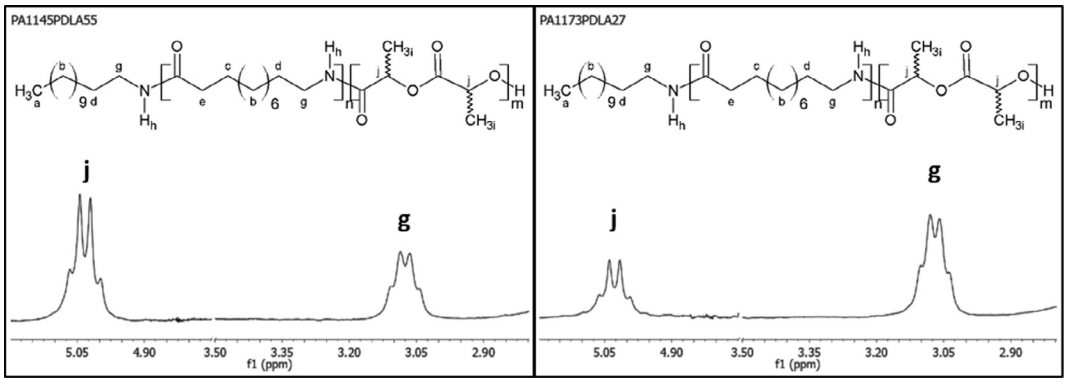

Fig. 3. ^{1}H NMR spectra of the samples $PA11_{45}PDLA_{55}$ (left) and $PA11_{73}PDLA_{27}$ (right) – zoom in the regions at δ 5.2–4.75 and 3.5–2.8 ppm.

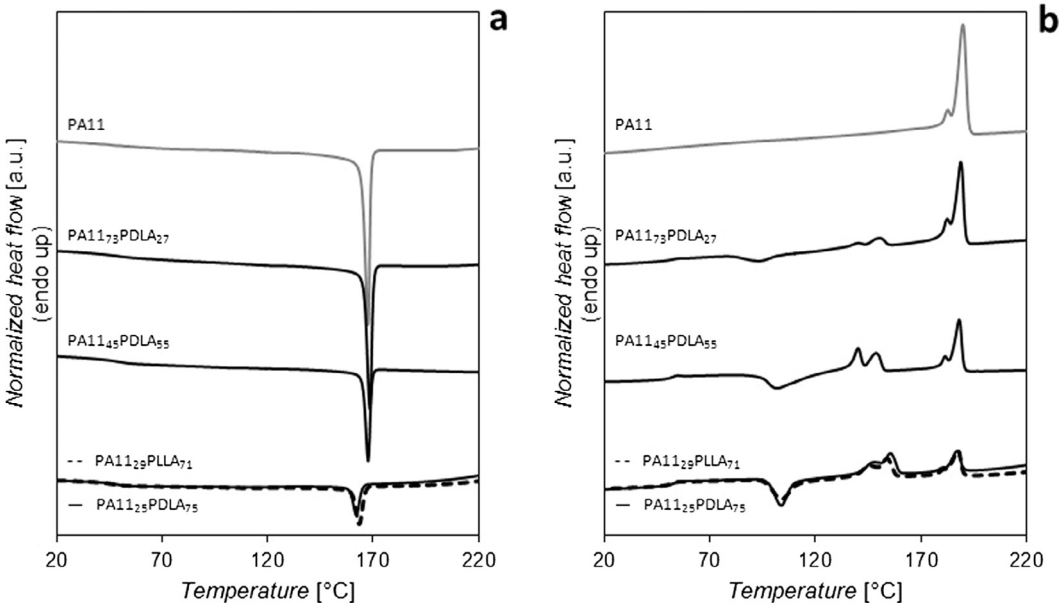

Fig. 4. DSC cooling (a) and subsequent heating (b) scans of the PA11$_x$PLA$_y$ diblock samples, together with those of the PA11 pre-polymer (grey lines), after 1-min relaxation in the melt at 230 °C.

relative intensities of the characteristic amide and ester carbonyl stretching bands. The corresponding TGA curves (Fig. 2b) display a double degradation step, the high-temperature one (with T_{max} at ~470 °C) ascribable to the polyamide segment, and a low-temperature one (with T_{max} in the range 300–350 °C) to be assigned to PLA. The relative ratio of the two steps reflects the block weight ratio in the copolymer (data given in Table 1). Indeed, a perfect consistency between the information derived from FTIR (qualitative), ^{1}H NMR and TGA measurements, about the copolymer composition, can be pointed out.

The molecular characteristics of the synthesized di-block copolymer samples are summarized in Table 1: by means of ROP of D-LA, where the conversion was controlled through the catalyst concentration, using the amino-terminated polyamide 11 ($M_n \sim 13 * 10^3$ g/mol) as macro-initiator, three different PA11$_x$PDLA$_y$ di-block copolymers were targeted, having a PA11:PDLA weight ratio of ~25:75, 45:55 and 73:27. These correspond to overall molecular weights of $\sim 52 \cdot 10^3$, $30 \cdot 10^3$ and $18 \cdot 10^3$ g/mol, respectively, which, actually, nicely comply with the different physical form of the samples (namely, more “fibrous-like” or powder-like). Based on the lactide monomer conversion (as measured by ^{1}H NMR spectroscopy, see Table 1), and having in mind that all polymerizations were carried out from a LA/PA11 3/1 (w/w) feed, the theoretical molecular weight for the three copolymers can be calculated (equating the mean degree of polymerization of the PLA block to the monomer conversion times the monomer-to-initiator ratio) as $\sim 50 \cdot 10^3$, $\sim 31 \cdot 10^3$ and $\sim 20 \cdot 10^3$ g/mol for PA11$_{25}$PDLA$_{75}$, PA11$_{45}$PDLA$_{55}$ and PA11$_{73}$PDLA$_{27}$, respectively. The very good agreement between the theoretical and experimental values (see Table 1) points out that the employed polymerization conditions are appropriate for the aminolytic ROP of lactide initiated by PA11 to be a living/well-controlled process. Incidentally, this evidence is a further proof for diblock copolymer formation, as it endorses the amino-terminated PA11 pre-polymer as a quantitative initiator.

Finally, the ROP of L-LA was carried out for 15 min with a [PA11]/[Sn(Oct)$_2$] ratio of 2.5, to prepare a PA11$_x$PLA$_y$ copolymer having characteristics similar to the sample PA11$_{25}$PDLA$_{75}$ (entry PA11$_{29}$PLLA$_{71}$ in Table 1; FTIR spectrum and TGA curve shown in Fig. 2).

The thermal properties of the PA11$_x$PLA$_y$ samples, as evaluated by means of DSC, are summarized in Table 2, while the corresponding cooling and heating curves are shown in Fig. 4. It is needed to underline that herein it is just presented a preliminary characterization of the materials, whereas more detailed studies will follow to give a better insight into the complex behavior of these double-crystalline diblock copolymers, also with respect to the polymorphism featured by both components. For all samples, only one clear glass transition could be detected, at ~52 °C, assigned to the PLA segment. Indeed, given the immiscible nature of the two polymers according to the literature [3], it

Table 2
Thermal properties of the PA11 pre-polymer and PA11$_x$PLA$_y$ diblock copolymers.

	Cooling[a]				2nd heating[a]						
Sample	T_c (h) [°C]	X_c[b] (h) [%]	T_c (PA) [°C]	X_c[b] (PA) [%]	T_g [°C]	T_{cc} (h) [°C]	X_{cc}[b] (h) [%]	T_m[c] (h) [°C]	X_m[b] (h) [%]	T_m[c] (PA) [°C]	X_m[b] (PA) [%]
PA11	–	–	167.6	31	45	–	–	–	–	182.8, 189.8	32
PA11$_{25}$PDLA$_{75}$	112.8	< 1 (1)	162.0	5 (21)	52	103.7	21 (28)	148.0, 155.5	21 (28)	180.0, 187.1	6 (22)
PA11$_{29}$PLLA$_{71}$	111.7	< 1 (1)	163.5	7 (26)	52	104.3	20 (28)	146.0, 153.8	20 (28)	180.5, 187.3	7 (26)
PA11$_{45}$PDLA$_{55}$	–	–	167.4	13 (29)	52	102.0	20 (37)	140.2, 148.7	20 (37)	181.5, 188.0	14 (29)
PA11$_{73}$PDLA$_{27}$	–	–	168.5	22 (30)	52	93.4	8 (31)	139.5, 150.1	9 (32)	182.5, 188.7	22 (30)

[a] Cooling scan, after melting at 230 °C for 1 min, and subsequent heating of the melt-cooled samples (from −10 °C to 230 °C); the subscripts c, cc and m indicate the values measured during crystallization, cold-crystallization and melting, respectively; (h) and (PA) indicate that the thermal transition was assigned either to (homocrystal) PLA or to PA11, respectively.

[b] X is the percentage of crystallinity, over the total weight of the sample, calculated by assuming ideal enthalpies of fusion of 93 J/g and 189 J/g for PLA homochiral crystals and PA11, respectively [15,18]; the values in brackets represent the degree of crystallinity normalized to the PLA/PA11 content (in g/g) as estimated by ^{1}H NMR.

[c] The two values signify the presence of a bimodal melting endotherm, whose peaks could be fairly discerned (the first value is related to the lower-temperature peak, the second one corresponds to the higher-temperature maximum).

is speculate that a second, distinct glass transition event, belonging to the PA11 block, is also present, just too weak to be discerned (as already difficult in the case of the PA11 homopolymer), also because of the close proximity of the two transition steps, causing partial overlapping. According to the cooling curves (Fig. 4a), PA11 always affords melt-crystallization regardless of its incorporation and amount in the copolymer. Nevertheless, a slight disturbance to its structuring, caused by the molten covalently bound PLA segment, can be pointed out in that both the crystallization temperature and extent of crystallinity experience a (modest) reduction with increasing the PLA fraction in the chain (see Table 2). The almost complete invariance of the PA11 melting temperature (*i.e.*, $T_m \sim 188\,^{\circ}C$) confirms the substantial immiscibility between the two blocks. Unlike PA11, the PLA segment cannot crystallize during cooling, with the exception of the PLA-richer samples $PA11_{25}PDLA_{75}$ and $PA11_{21}PLLA_{79}$, for which a very minute exotherm (not visible on the scale of Fig. 4a) can be detected around 110 °C – at this stage, however, it is not possible to rule out that this tiny crystallization event belongs to PA11, undergoing fractionated crystallization as a consequence of the confinement in isolated microdomains. The absence of any significant PLA crystallization on melt-cooling is particularly remarkable given the relatively low molecular weight of the PLA segment in our samples (corroborated by their powder/flake-like form), which should favor the crystallization kinetics. Indeed, this evidence suggests a depression of the crystallizability of the PLA block, reasonably ascribable to the constraints imposed by the first-formed PA11 crystals. Thus, the PLA block is able to crystallize just upon subsequent heating, *i.e.*, from the glassy state, the cold-crystallization peak being around 90–100 °C for all the samples (see Table 2 – the easiness of structuring seemingly being dictated by the chain lenght/mobility). The ~8–20% (over the total weight of the sample; ~ 30% relative to the PLA fraction) of PLA homo-crystallites formed on heating subsequently melts in the range ~140–155 °C, always exhibiting a bimodal melting peak. The presence of multimodal melting endotherms is typical of polyesters, and it is generally attributed to reorganization processes (that is, melting and recrystallization/perfection) during the scan [26,27]. In the specific case of PLLA, some authors have ascribed the low-temperature peak to the melting of the more defective α′ crystals, and the high-temperature one to the more stable α polymorph of PLLA [28]. A slight upward shift of the PLA melting peaks with increasing the PLA content in the copolymer (that is, the length of the PLA chain) can be recognized, in agreement with the general dependence of the melting temperature on crystal thickness.

As a further step, one wanted to establish stereocomplexation of the $PA11_xPLA_y$ diblock copolymers. In fact, stereocomplex formation was reported in a number of PLLA/PDLA-containing block copolymers, apparently regardless of the nature – miscible or immiscible – of the block conjugated to the PLA blocks [29–37]. For the purpose, the two enantiomeric samples $PA11_{25}PDLA_{75}$ and $PA11_{21}PLLA_{79}$, having similar composition and the longer PLA block (*i.e.*, approximately $35 \cdot 10^3$ g/mol), were melt-blended in equimolar amount as described in the Experimental Section (sample $PA11_{23}LD_{77}$). Indeed, the DSC heating scan of the as-prepared blend (grey curve in Fig. 5) displays, together with a glass transition step at ~52 °C, two melting peaks at 186 °C and 207 °C. By comparison with the thermograms of the two non-blended partners, the first peak can be assigned to the melting of PA11, whereas the second one, appearing at higher temperature than both homocrystal PLA and PA11 melting endotherms, needs to be related to the formation of stereocomplex PLA, which is known from the literature to have a melting point up to 50 °C higher than that of the two single homopolymers [15]. It is of the utmost relevance that no trace of melting of either PLLA or PDLA homo-crystallites can be discerned, nor any cold-crystallization event: that is, in spite of the fast cooling of the blend (thence short crystallization time enabled), the PLA segments were quickly (and exclusively) involved in the formation of the stereocomplex, to give a material made up of ~7% of PA11 crystals and ~20% of stereocomplex crystallites. The same results were obtained by

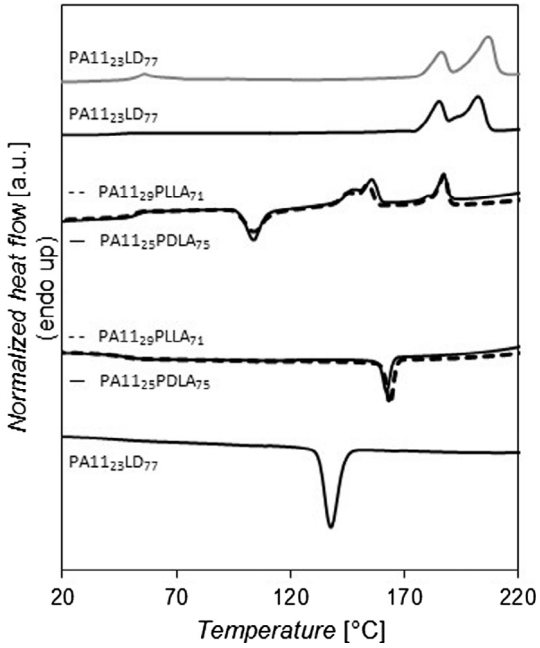

Fig. 5. DSC cooling and subsequent heating thermograms (lower and upper curves, respectively) of the sample $PA11_{23}LD_{77}$, after 1-min melt-relaxation at 230 °C, as compared to the two non-blended partners (samples $PA11_{25}PLLA_{75}$ and $PA11_{21}PDLA_{79}$). The grey curve represents the first heating scan of the as-prepared $PA11_{23}LD_{77}$ blend.

slowly cooling the blend at 10 °C/min after 1-min holding in the melt at 230 °C (black upper curve): in this case, the melting peak of the stereocomplex is shifted to 202 °C, thus the two endotherms are partially overlapped, however, the overall melting enthalpy is unaffected. Interestingly, the cooling curve of the sample $PA11_{23}LD_{77}$ shows a single crystallization exotherm (at 138 °C), whose integral area corresponds exactly to that of the two melting peaks. This means that PA11 and the stereocomplex crystallize "concomitantly", at a temperature which is even lower than that of crystallization of the neat PA11 homopolymer. Similar findings were reported for poly(ethylene) (PE)-PLLA di-block copolymers, where, due to the strong segregation strength of the melt, the PLLA crystallization process was found to be strongly delayed, up to the point of overlapping with that of PE at lower temperatures [38]. However, in that case, the coincident crystallization was occurring few degrees below that of homo-PE, whereas in our case also the crystallization of the PA11 block is severely depressed – indeed, in the literature case, a nucleating effect of the first-crystallized PLLA on PE was disclosed, partially compensating the topological restrictions imposed by the crystalline framework, which may not be true for our copolymers.

WAXD was used to determine/confirm the crystalline structure of the diblock and blend samples. Fig. 6 shows the WAXD patterns of $PA11_{25}PDLA_{75}$ (as-precipitated) and $PA11_{23}LD_{77}$ (as-prepared). Indeed, when first considering the diffractions associated with the PLA segment, it can be seen that the enantiomeric diblock $PA11_{25}PDLA_{75}$ contains all the diffraction peaks assigned to the α-form of homo-crystals, with the main peaks at scattering angles of $2\theta \sim 15$, 17, and 19° [15,39]. Conversely, the $PA11_{23}LD_{77}$ blend exhibits the characteristic peaks of the stereocomplex crystallites at $2\theta \sim 12$, 21, and 24° alone [15], thus corroborating the exclusive stereocomplex formation. As for the PA11 block, while the as-precipitated diblock $PA11_{25}PDLA_{75}$ displays the typical peaks for the triclinic α-form of PA11 at $2\theta \sim 20$ and 23.5°, the as-prepared $PA11_{23}LD_{77}$ blend contains a sole broad reflection at $2\theta \sim 21.6°$, indicative of the formation of the kinetically-favored pseudo-hexagonal smectic-like δ′-phase, as expected for fast melt cooling (typically, it is produced by quenching the melt into an ice bath) [18,22,40]. The melt-quenched δ′-form is known for its piezoelectric properties.

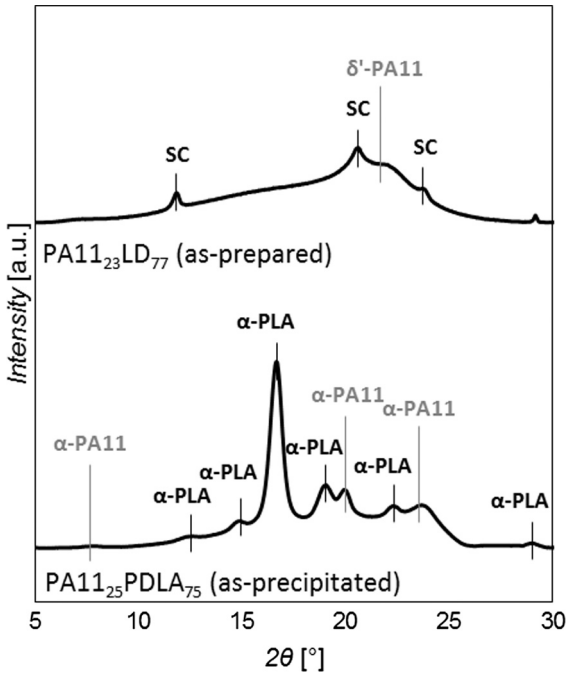

Fig. 6. WAXD profiles of the (as-precipitated) di-block copolymer $PA11_{25}PLLA_{75}$ (bottom) and of the (as-prepared) blend $PA11_{23}LD_{77}$ (top curve).

From the above (qualitative) observations, it is evident the need for further and deeper inquiries into the ordering behavior of these novel materials, also in the interesting perspective to template, in turn, the crystallization of either the PLA or PA11 block (in fact, the melting temperature of PA11 lies exactly between those of PLA homo-crystals and stereocomplex PLA), which may, for example, affect polymorphism. Such investigation will be performed in the near future.

4. Conclusions

In the present work, it is reported on the preparation of novel, fully bio-based $PA11_xPLA_y$ diblock copolymers. The adopted synthetic strategy relied on the synthesis of an amino-terminated PA11 prepolymer (*i.e.*, having the amino end group available and the carboxylic one protected), to be employed subsequently as a macro-initiator in the ROP of D-lactide (or L-lactide). Following the first step polycondensation of 11-aminoundecanoic acid using dodecylamine as a chain terminating agent, a PA11 product with $M_n \sim 13{\cdot}10^3$ g/mol and the majority of the chains effectively having the sole amino end group free was prepared, as ascertained by ^{1}H NMR spectroscopy and MALDI-TOF mass spectrometry, respectively. Thereafter, the as-synthesized PA11 prepolymer was mixed with 3 parts by mass of D-lactide, whereby the aminolytic ROP was conducted at a temperature of 185 °C (namely, below that of melting of PA11, the molten lactide acting as a solvent for PA11), from a homogeneous liquid phase. Due to miscibility issues, the 3:1 monomer-to-initiator ratio in the feed was kept fixed, thence the composition of the diblocks (that is, the length of the PDLA block) needed to be varied by tuning the lactide conversion, which was accomplished through the catalyst concentration. As determined by ^{1}H NMR and TGA analyses, three different $PA11_xPDLA_y$ diblocks were successfully targeted, having a PA11:PDLA weight ratio of ~25:75, 45:55 and 73:27 (corresponding to overall molecular weights of $\sim 50 \cdot 10^3$, $30 \cdot 10^3$ and $20 \cdot 10^3$ g/mol, respectively). A PLA-rich (that is, PA11:PLA ~ 29:71) $PA11_xPLLA_y$ copolymer was also synthesized starting from L-LA. ^{1}H NMR spectroscopy confirmed the quantitative initiation of the ROP of lactide by PA11, thence the co-polymeric nature of our products.

A (preliminary) study of the complex thermal behavior of the obtained double-crystalline diblock copolymers was performed by means of DSC. Most important, PLA stereocomplexation was demonstrated upon equimolarly mixing the two enantiomeric $PA11_xPDLA_y$/$PA11_xPLLA_y$ diblocks having similar composition (that is, PA11:PLA ~ 25:75), indeed finding that the PLA segments are quickly (and exclusively) involved in the formation of the stereocomplex, even in the case of fast cooling (quenching) from the melt.

Clearly, the appeal of these systems mainly holds from a factual point, in that it was fabricated completely renewable materials conjugating the properties of PLA with those of the high-performance, high-impact PA11, in a cumulative rather than intermediate fashion as for random poly(ester amide)s, but without phase separation occurring as for PLA/PA11 immiscible blends. In addition, the presence of the stereocomplex imparts even further quality. For example, it was imagined to introduce the $PA11_xPDLA_y$ copolymers into a commercial PLLA, which is expected to result in tough (possibly piezoelectric) PA11 domains dispersed in the PLA matrix, with the stereocomplex regions acting as a strong link between the two. Furthermore, the application of the diblocks as compatibilizers for PA11/PLA blends can be envisaged. In addition, these systems are highly interesting also from a more "theoretical" point of view, as they offer the possibility to template/confine, in turn, the crystallization of either the PLA or the PA11 block, the melting temperature of PA11 falling exactly between those of PLA homocrystals and sc-PLA.

Acknowledgements

This research did not receive any specific grant from funding agencies in the public, commercial, or not-for-profit sectors.

Appendix A. Supplementary material

Supplementary data associated with this article can be found, in the online version, at http://dx.doi.org/10.1016/j.eurpolymj.2017.11.008.

References

[1] D. Garlotta, A literature review of poly(lactic acid), J. Polym. Environ. 63 (2002) 63–84.
[2] J.E. Mark (Ed.), Polymer Data Handbook, Oxford University Press, Inc., New York, 1999.
[3] G. Stoclet, R. Seguela, J.-M. Lefebvre, Morphology, thermal behavior and mechanical properties of binary blends of compatible biosourced polymers: polylactide/polyamide11, Polymer 52 (2011) 1417–1425.
[4] R. Patel, D.A. Ruehle, J.R. Dorgan, P. Halley, D. Martin, Biorenewable blends of polyamide-11 and polylactide, Polym. Eng. Sci. 54 (2014) 1523–1532.
[5] A. Nuzzo, S. Coiai, S.C. Carroccio, N.T. Dintcheva, C. Gambarotti, G. Filippone, Heat-resistant fully bio-based nanocomposite blends based on poly(lactic acid), Macromol. Mater. Eng. 299 (2014) 31–40.
[6] A. Nuzzo, E. Bilotti, T. Peijs, D. Acierno, G. Filippone, G., Nanoparticle-induced co-continuity in immiscible polymer blends – a comparative study on bio-based PLA-PA11 blends filled with organoclay, sepiolite, and carbon nanotubes, Polymer 55 (2014) 4908–4919.
[7] W. Dong, X. Cao, Y. Li, High-performance biosourced poly(lactic acid)/polyamide 11 blends with controlled salami structure, Polym. Int. 63 (2014) 1094–1100.
[8] Q. Zhiyong, L. Sai, Z. Hailian, L. Xiaobo, Synthesis, characterization and in vitro degradation of biodegradable polyesteramide based on lactic acid, Colloid Polym. Sci. 281 (2003) 869–875.
[9] Y.P. Ge, D. Yuan, Z.L. Luo, B.B. Wang, Synthesis and characterization of poly(ester amide) from renewable resources through melt polycondensation, Express Polym. Lett. 8 (2014) 50–54.
[10] G. Deshayes, C. Delcourt, I. Verbruggen, L. Trouillet-Fonti, F. Touraud, E. Fleury, P. Degée, M. Destarac, R. Willem, P. Dubois, Activation of the hydrolytic polymerization of e-caprolactam by ester functions: straightforward route to aliphatic polyesteramides, React Funct. Polym. 68 (2008) 1392–1407.
[11] R.M. Michell, A.J. Müller, V. Castelletto, I. Hamley, G. Deshayes, P. Dubois, Effect of sequence distribution on the morphology, crystallization, melting, and biodegradation of poly(ε-caprolactone-co-ε-caprolactam) copolymers, Macromolecules 42 (2009) 6671–6681.
[12] G. Deshayes, C. Delcourt, I. Verbruggen, L. Trouillet-Fonti, F. Touraud, E. Fleury, P. Degée, M. Destarac, R. Willem, P. Dubois, Novel polyesteramide-based di- and triblock copolymers: from thermo-mechanical properties to hydrolytic degradation, Eur. Polym. J. 47 (2011) 98–100.
[13] J.I. Scheinbeim, Piezoelectricity in gamma-form nylon-11, J. Appl. Phys. 52 (1981)

5939–5942.
[14] S.L. Wu, J.I. Scheinbeim, B.A. Newman, Ferroelectricity and piezoelectricity of nylon 11 films with different draw ratios, J. Polym. Sci., Part B: Polym. Phys. 37 (1999) 2737–2746.
[15] H. Tsuji, Poly(lactide) stereocomplexes: formation, structure, properties, degradation, and applications, Macromol. Biosci. 5 (2005) 569–597.
[16] E. Jacobi, H. Schuttenberg, R.C. Schulz, A new method for gel permeation chromatography of polyamides, Makromol. Chem., Rapid Commun. 1 (1980) 397–402.
[17] E.C. Robert, R. Bruessau, J. Dubois, B. Jacques, N. Meijerink, T.Q. Nguyen, D.E. Niehaus, W.A. Tobisch, Characterization of polyamides 6, 11, and 12: determination of molecular weight by size exclusion chromatography, Pure Appl. Chem. 76 (2009) 2009–2025.
[18] A. Mollova, R. Androsch, D. Mileva, C. Schick, A. Benhamida, Effect of supercooling on crystallization of polyamide 11, Macromolecules 46 (2013) 828–835.
[19] P.M. Lloyd, K.G. Suddaby, J.E. Varney, E. Scrivener, P.J. Derrick, D.M. Haddleton, A comparison between matrix-assisted laser desorption/ionisation time-of-flight mass spectrometry and size exclusion chromatography in the mass characterisation of synthetic polymers with narrow molecular-mass distributions: poly(methyl methacrylate) and poly(styrene), Eur. Mass Spectrom. 1 (1995) 293–300.
[20] S.V. Levchik, L. Costa, G. Camino, Effect of the fire-retardant, ammonium polyphosphate, on the thermal decomposition of aliphatic polyamides. I. Polyamides 11 and 12, Polym. Degrad. Stab. 36 (1992) 31–41.
[21] S.V. Levchik, E.D. Weil, M. Lewin, Thermal decomposition of aliphatic nylons, Polym. Int. 48 (1999) 532–557.
[22] S. Gogolewski, Effect of annealing on thermal properties and crystalline structure of polyamides. Nylon 11 (polyundecaneamide), Colloid Polym Sci 257 (1979) 811–819.
[23] P. Degée, P. Dubois, S. Jacobsen, H.G. Fritz, R. Jérôme, Beneficial effect of triphenylphosphine on the bulk polymerization of L,L-lactide promoted by 2-ethylhexanoic acid tin (II) salt, J. Polym. Sci., Part A: Polym. Chem. 37 (1999) 2413–2420.
[24] R.D. Davis, W.L. Jarrett, L.J. Mathias, Solution ^{13}C NMR spectroscopy of polyamide homopolymers (nylons 6, 11, 12, 66, 69, 610 and 612) and several commercial copolymers, Polymer 42 (2001) 2621–2626.
[25] H.R. Kricheldorf, J.M. Jonte, M. Berl, Polylactone 3. Copolymerization of glycolide with DL-lactide and other lactones, Makromol. Chem. Suppl. 12 (1985) 25–38.
[26] X. Ling, J.E. Spruiell, Analysis of the complex thermal behavior of poly(L-lactic acid) film. II. Samples crystallized from the melt, J. Polym. Sci., Part B: Polym. Phys. 44 (2006) 3200–3214.
[27] M.L. Di Lorenzo, Calorimetric analysis of the multiple melting behavior of poly(L-lactic acid), J. Appl. Polym. Sci. 100 (2006) 3145–3151.
[28] J. Zhang, K. Tashiro, H. Tsuji, A.J. Domb, Disorder-to-order phase transition and multiple melting behavior of poly(L-lactide) investigated by simultaneous measurements of WAXD and DSC, Macromolecules 41 (2008) 1352–1357.
[29] S. Pensec, M. Leory, H. Akkouche, N. Spassky, Stereocomplex formation in enantiomeric diblock and triblock copolymers of poly(ε-caprolactone) and polylactide, Polym. Bull. 45 (2000) 373–380.
[30] R. Slivniak, A.J. Domb, Stereocomplexes of enantiomeric lactic acid and sebacic acid ester-anhydride triblock copolymers, Biomacromolecules 3 (2002) 754–760.
[31] S. Li, M. Vert, Synthesis, characterization, and stereocomplex-induced gelation of block copolymers prepared by ring-opening polymerization of L(D)-lactide in the presence of poly(ethylene glycol), Macromolecules 36 (2003) 8008–8014.
[32] N. Kang, M.E. Perron, E.E. Prud'homme, Y. Zhang, G. Gaucher, J.C. Leroux, Stereocomplex block copolymer micelles: core – shell nanostructures with enhanced stability, Nano Lett. 5 (2005) 315–319.
[33] Z. Zhang, D.W. Grijpma, J. Feijen, Triblock copolymers based on 1,3-trimethylene carbonate and lactide as biodegradable thermoplastic elastomers, Macromol. Chem. Phys. 205 (2004) 867–875.
[34] H.R. Kricheldorf, S. Rost, C. Wutz, A. Domb, Stereocomplexes of A-B-A triblock copolymers based on poly(L-lactide) and poly(D-lactide) A blocks, Macromolecules 38 (2005) 7018–7025.
[35] L. Jia, L. Yin, Y. Li, Q. Li, J. Yang, J. Yu, Z. Shi, Q. Fang, A. Cao, New enantiomeric polylactide-block-poly(butylene succinate)-block-polylactides: syntheses, characterization and in situ self-assembly, Macromol. Biosci. 5 (2005) 526–538.
[36] C.L. Wanamaker, W.B. Tolman, M.A. Hillmyer, consequences of polylactide stereochemistry on the properties of polylactide-polymenthide-polylactide thermoplastic elastomers, Biomacromolecules 10 (2009) 2904–2911.
[37] R.M. Michell, A.J. Müller, M. Spasova, P. Dubois, S. Burattini, B.W. Greenland, I.W. Hamley, D. Hermida-Merino, N. Cheval, A. Fahmi, Crystallization and stereocomplexation behavior of poly(D- and L-lactide)-b-poly(N, N-dimethylamino-2-ethyl methacrylate) block copolymers, J. Polym. Sci., Part B: Polym. Phys. 49 (2011) 1397–1409.
[38] R.V. Castillo, A.J. Müller, M.C. Lin, H.L. Chen, U.S. Jeng, M.A. Hillmyer, Confined crystallization and morphology of melt segregated PLLA-b-PE and PLDA-b-PE diblock copolymers, Macromolecules 41 (2008) 6154–6164.
[39] Pengju Pan, Bo Zhu, Weihua Kai, Tungalag Dong, Yoshio Inoue, Effect of crystallization temperature on crystal modifications and crystallization kinetics of poly(L-lactide), J. Appl. Polym. Sci. 107 (2008) 54–62.
[40] Qingxin Zhang, Zhishen Mo, Hongfang Zhang, Siyang Liu, S.Z.D. Cheng, Crystal transitions of Nylon 11 under drawing and annealing, Polymer 42 (2001) 5543–5547.